ingegneria sismica
International Journal of Earthquake Engineering
Anno XLIII - Num. 2 - 2026

Study on fault node monitoring of power distribution network based on genetic algorithm with improved software defined rules

Wenqang Zou[1,*], *Kunhua Yang*[1], *Yuchuan Deng*[1], *Xuan'an Lin*[1] *and Ying Deng*[1]

[1] Guiyang Power Supply Bureau of Guizhou Power Grid Co., Ltd., Guiyang, Guizhou, 550001, China

SUMMARY: *In this paper, based on OpenFlow technology for software-defined networks, a QoS-ensure flow control strategy consisting of modules such as fault monitoring and QoS routing control is proposed. After that, a real-time route planning framework based on software-defined network (SDN) is designed, and then a QoS route planning method based on adaptive genetic ant colony is proposed by combining the characteristics of genetic algorithm and ant colony algorithm. Aiming at the problem of poor adaptability and anti-interference of genetic algorithm, an optimized genetic algorithm for fault node localization in power distribution network is proposed. Simulation results show that the adaptive genetic algorithm proposed in this paper can obtain better search performance than the max-min ant system and the basic ant colony algorithm, and it can search for routing solutions with lower cost than the traditional algorithms, but its convergence performance is a little worse than the max-min ant system. The improved genetic algorithm (IBPSO) in this paper can quickly and accurately locate faulty segments under multiple fault scenarios, such as single fault, multipoint fault, and end-of-feeder fault in the network, and it has strong fault-tolerance performance when the fault information is distorted.*

KEYWORDS: *QoS; SDN; AGAC algorithm; power distribution network; fault node monitoring*

1 Introduction

In the industrialized and information society, power grid is the foundation and important part of social development. With the development of technology and the increasing requirements of the country and people on the quality of power supply, countries continue to promote the construction of power grids [1]. With the gradual construction of the power grid, the distribution network gradually embodies the characteristics of long lines, many branches, complex structure, susceptible to external forces and the natural environment, resulting in the distribution network is very prone to failure [2]. When a line fault occurs through the program for fault isolation automation processing, to prevent the expansion of the scope of the fault, to guide the staff to find and deal with the fault point in a timely manner, which can reduce the difficulty of fault point investigation, thereby reducing economic losses, speeding up the recovery of power supply, and improving the reliability of power supply.

In recent years, many scholars at home and abroad have devoted themselves to the research of fault node monitoring technology in distribution networks, proposed some solutions and achieved certain results. However, the vast majority of methods are based on the fault current

*zouwenqiang763@163.com
https://doi.org/10.65102/is2026701 Published: 30 April, 2026

collected by the feeder terminal unit on the MV side for localization and monitoring, which can only locate the fault in the area surrounded by the feeder terminal unit, due to the long distance between adjacent feeder terminal units [3]. Therefore, after determining the fault section, it still takes a long time to find the specific location of the fault. At present, the research on fault node monitoring technology for distribution networks is mainly divided into the following categories:

(1) Matrix method: The matrix method derives the fault discrimination matrix by writing the network topology matrix and the fault information matrix, i.e., whether the corresponding node flows a short-circuit current or not, so as to monitor and locate the faults [4]. For example, Wang, C et al. proposed a fast distribution network reliability calculation method based on fault correlation matrix by constructing a M-segment-N contact switch reliability calculation unit suitable for complex distribution networks and obtaining the inverse matrix of its node-branch correlation matrix to obtain the power supply path matrix, which then establishes three types of fault correlation matrices according to the different types of impacts of the fault event on the load points [5]. However, the principle of the matrix method is simple and the computational load is small, but it is only applicable to simple networks; for complex networks, the computational load is too large, so it is not applicable to complex networks. Therefore, many scholars have improved the matrix method. For example, Li, Z et al. proposed a collaborative positioning method that integrates the improved matrix algorithm and the optimization algorithm. It establishes the causal relationship between the alarm information and the fault section through the matrix algorithm to generate hypotheses, and uses network segmentation to verify the causality; if the alarm information is normal, the fault can be directly and quickly located; if the information is distorted, an optimization model is constructed based on the hypotheses selected by the matrix algorithm, and the real fault section is solved using the discrete particle swarm optimization algorithm [6].

(2) Impedance method: the principle of the impedance method is to obtain the electrical distance from the bus terminal to the fault point by measuring the voltage and current, so as to derive the impedance corresponding to the fault point, and to locate the fault through the positive proportionality between the impedance and the distance [7]. For example, Hosseinimoghadam, S et al. proposed an impedance matrix method based on impedance matrix method for fault localization in distribution networks containing distributed power sources, which has higher speed and accuracy in fault localization compared to the traditional matrix method and can still be accurately located when the network is asymmetrical [8]. Hamatwi, E et al. compared the performance of three high impedance fault detection techniques, discrete Fourier transform, discrete wavelet transform and power spectral analysis, in distribution networks and found that the power spectral analysis technique performs optimally in high impedance fault detection with 100% accuracy, shorter processing time and larger fault detection margin, which is the most suitable for the high impedance fault detection needs of distribution networks [9]. Mortazavi, H et al. proposed an apparent impedance-based distribution network monitoring method, which calculates apparent impedance by measuring bus voltage and injected current, and utilizes its variation in the R-X plane to monitor key electrical quantities such as feeder power factor, active and reactive power extremes, etc., in real time, which is applicable to complex scenarios such as unbalanced loads, distributed and centralized photovoltaics, and wind power access [10].

(3) Traveling wave method: the traveling wave method is based on the principle that the fault distance is proportional to the travelling wave transmission time, specifically the use of transient travelling waves in the line after folding and reflecting the propagation to the device measurement point of the moment and the corresponding travelling wave speed for fault monitoring [11]. Kong, B et al. proposed a method for fault monitoring in distribution networks using traveling waves which is analyzed using image processing method which uses voltage

information from all nodes to create a voltage image and analyzes the traveling wave data with dynamic changes in the image to determine the location of the fault [12]. Qin, X et al. proposed a distribution line fault type identification method based on the time-frequency characteristics of fault waveforms, which realizes the automatic classification of fault types caused by multiple factors by analyzing the time-domain, frequency-domain, and arc characteristics of different fault waveforms, extracting multi-dimensional feature parameters, and establishing a multi-parameter fusion identification logic [13]. Izadi, M and Mohsenian-Rad, H proposed a method for synchronously locating transient events in the power distribution system using waveform measurement units. This method extracts the oscillation patterns of the transient components in the synchronous voltage and current waveforms of each WMU (Waveform Measurement Unit) through multi-signal modal analysis. An equivalent circuit model corresponding to the power distribution line is constructed based on the dominant frequency, and transient event location is achieved through forward-backward analysis [14]. However, due to the many branches of the distribution network and the discontinuity of the wave impedance of the mixed lines, it is more difficult to recognize the folded reflected traveling wave, which makes it difficult to determine the moment of arrival of the initial reflected wave at the fault point, thus limiting the application of the traveling wave method in the distribution system.

(4) Bayesian method: the Bayesian method is based on the probability of fault location, that is, the use of information collected on the distribution line, and this information is transmitted back to the data centralized control center through the transmission system, using the network topology information as well as the Bayesian formula for the analysis, to determine the area with the highest probability as the fault area [15]. Zhu, J et al. used the wavelet energy ratio, wavelet coefficient variance and wavelet power obtained from fault transient component decomposition to construct feature vectors, and by comparing the three parameter tuning algorithms, the Bayesian optimization algorithm was chosen to achieve adaptive tuning of model parameters [16]. Cai, B et al. proposed a dynamic Bayesian network (DBN)-based approach for diagnosing transient and intermittent faults in electronic systems. The dynamic degradation process of electronic products is modeled by DBN and Markov chain is used to describe the transfer relationship between four states: no fault, transient fault, intermittent fault and permanent fault [17]. Jiang, K et al. proposed a new method for active distribution network fault localization based on finite synchronous phasor measurement units, which transforms the fault localization problem into an estimation problem of block sparse fault injection current signals, which is solved by an improved block sparse Bayesian learning algorithm by exploiting the block structure of the signals with the intra-block correlation [18]. Wang, Y et al. proposed a faulty segment localization method based on impulse neural P system with Bayesian estimation, which decouples the distribution network topology into a single-branch network, uses impulse neural P system with excitatory/inhibitory synapses to model the suspected faulty segments, and obtains the initial localization results through a matrix inference algorithm; subsequently, it combines the Bayesian estimation with the principle of contradiction to validate and correct the initial results, and obtains the final localization results [19]. The Bayesian method is easy to apply and has good real-time performance, but it can only be used for fault localization in approximate segments, and this method requires the support of many previous operational fault data of the power grid to be realized.

(5) Distribution network fault monitoring methods based on machine learning algorithms: the core logic of the machine learning approach is to consider distribution network fault monitoring as a data-driven pattern recognition and prediction problem, which can be continuously adapted to network structure changes and operation mode adjustments through learning [20]. For example, Mirshekali, H et al. proposed a machine-learning based fault monitoring method for distribution networks, which utilizes the voltage data recorded by the

micro-phase volume measurement unit during the fault period by extracting the frequency components of the voltage signal as feature vectors, combining with the neighborhood component feature selection algorithm for feature dimensionality reduction, and using a support vector machine classifier to achieve the fault section identification [21]. Baghaee, H et al. proposed a machine learning method based on support vector machines for improved islanding detection and grid fault identification and monitoring in photovoltaic systems [22]. Rizeakos, V et al. proposed a data-driven fault location and type classification method based on continuous wavelet transform and convolutional neural network, and model hyper-parameter tuning through Bayesian optimization. The method utilizes high-precision measurement equipment data of distribution networks to extract spatial features and frequency domain time domain features of three-phase voltage and current time series signals, which can achieve precise location of short-circuit faults and accurate classification of 11 fault types [23]. Maruf, H et al. proposed a multi-step machine learning fusion based fault classification and identification method for distribution networks, which performs fault diagnosis in three steps (fault phase classification, impedance level detection and faulty line segment identification) by integrating artificial neural networks, support vector machines, bagging trees and adaptive boosting algorithms to improve the overall accuracy by utilizing voltage and current measurements of feeders containing distributed power sources [24]. Although the above machine learning algorithms have high accuracy, however, they rely heavily on high-quality fault data, have complex models, and are computationally intensive, while only limited fault data can be obtained in the actual distribution network. Therefore, there are still some limitations in using machine learning algorithms for fault monitoring in practice.

(5) Intelligent algorithm-based fault monitoring methods for distribution networks: Intelligent algorithms refer to computational methods for solving complex problems by simulating natural processes or data-driven solutions, and contain traditional types such as simulated annealing, genetic algorithms, and forbidden searches, as well as group intelligent algorithms such as particle swarm optimization, and sparrow search [25]. For example, Bi, Z et al. applied the quantum annealing algorithm to the fault segment localization problem in distribution networks, and proposed an improved quantum annealing algorithm by constructing a quantum Hamiltonian function containing potential and kinetic energy terms, which showed excellent fault tolerance, global search capability and stability in complex scenarios, such as signal distortion and multiple fault segments [26]. Kahouli, O et al. proposed an optimization method for distribution network reconfiguration to reduce outage shortage and active losses as an objective function, combined with network operation constraints, and solved by using exhaustive, genetic and particle swarm optimization algorithms in comparison with the IEEE 33-node system [27]. Wen, J et al. proposed an active distribution network fault localization method based on dynamic quantum genetic algorithm, which measures the fault current code by feeder terminal unit, combines the generalized switching function to convert the switching state into the uploaded fault current code, and constructs the optimization objective function for the anti-false judgment factor [28]. Genetic algorithm is a random search probabilistic algorithm with high fault tolerance and good robustness. In the process of development, the genes of the organisms, through the evolution of generations, present a certain law and gradually change, forming the current state of the organisms, which is the fundamental idea of the genetic algorithm. In the distribution network fault location, the basic process of using genetic algorithm is to use the algorithm to find the maximum value of the objective function, the solution obtained at this time, is the fault location results [29].

This paper first designs the five major modules of the QoS traffic control strategy, namely "data monitoring, fault monitoring and QoS routing control"; then proposes an intelligent routing algorithm based on adaptive genetic ant colony (AGAC). This algorithm outputs the path through the genetic algorithm, uses the ant colony algorithm as the initial pheromone information, and takes advantage of the rapid global search ability of the genetic algorithm to accelerate the convergence speed of the AGAC algorithm and avoid the ant colony algorithm getting stuck in the local optimal solution state. Then according to the fault overcurrent signal detected by the FTU, the segment-based distribution network line state parameters are output, and then the parameter coding, switching function and adaptation function are optimized to improve the adaptability and anti-interference of fault location. Finally, the application effect of this fault location algorithm in fault node monitoring of power distribution network is verified through simulation analysis.

2 Software-defined rule-based routing design for grid data centers

2.1 Design related to QoS traffic control policies

2.1.1 Data monitoring module

Grid data center network often occurs in the network flow dynamic changes, so it is necessary to monitor the changes in traffic demand, and statistics on the corresponding link information, in order to equalize the flow and meet the needs of QoS. That is, the need to obtain dynamic information in real time, and targeted analysis and processing.

2.1.2 Fault monitoring module

The switch and the controller can communicate with each other with the help of Echo messages, and if the status of one side is normal, the Echo reply message will be sent to the other side. If the controller does not receive an Echo reply message from the switch within a set time interval, it determines that there is an anomaly between the two and updates the link information in the appropriate flow table entry. In addition, the controller removes the path from the list of potential shortest paths with the help of a routing algorithm.

2.1.3 QoS routing control module

The QoS route control module mainly accomplishes the collection, analysis and further processing of information. Among them, the collection of information is mainly realized through the invocation of other modules: the topological view of the network and the relevant link information collection is invoked by the routing link module; the collection of link load and the corresponding node-related information is invoked by the data monitoring module; and the acquisition of the network failure situation is invoked by the failure monitoring module. After the information collection is completed, the routing engine module makes decisions on the behavior of OpenFlow switches and provisioning on the basis of analyzing the data and optimizing the QoS information.

2.1.4 QoS Routing Engine Module

The QoS routing engine module is the core of the control strategy in this paper and is used for the realization of QoS-ensure traffic control strategy. The network topology consisting of communication links of each node can be denoted as $G(V,E)$. Where $V(E)$ represents the set of switches in the network. In addition, $S(D)$ denotes the source transmitter, P denotes the switch path between S and D, and U_{ij} and d_{ij} represent the available bandwidth of the link between i and j nodes and the previous delay, respectively. Finally, the bottleneck bandwidth $B(p)$ corresponding to path P and the corresponding delay jitter $D(p)$ are obtained:

$$\begin{cases} B(p) = \min u_{ij}, i, j \in V \\ D(p) = \sum_{i}^{n}\sum_{j}^{n} d_{ij}, i, j \in V \end{cases} \tag{1}$$

Using $R(p)$ to represent the network cost corresponding to the path P, it can be obtained:

$$R(p) = (1-\beta)D(p) + \beta S(p), \beta \in [0,1] \tag{2}$$

The $S(p)$ in Eq. represents the packet loss rate. The value of β is a constant, which is related to the delay jitter and packet loss rate, and its smaller value means that the stream has a higher delay jitter requirement and a lower packet loss rate requirement.

In addition, W_{ij} and $\bar{W}$ are used to represent the bandwidth utilization, average bandwidth utilization between nodes i and j, respectively, and F is used to represent the demanded bandwidth:

$$\begin{cases} W_{ij} = \dfrac{F}{U_{ij}} \\ \bar{W} = \dfrac{\sum_{i}^{n}\sum_{j}^{n} W_{ij}}{h(p)} \end{cases} \tag{3}$$

where $h(p)$ represents the number of links contained in the path P.

Further the variance corresponding to the path P can be obtained:

$$\delta^2 = \sum_{i}^{n}\sum_{j}^{n}\left(W_{ij} - \bar{W}\right)^2 \tag{4}$$

Ultimately, the constraints that must be satisfied by the objective to be optimized for the routing problem in this paper are:

$$\begin{cases} D(p) \le D \\ \min(R(p)) \\ \min(\delta^2) \end{cases} \tag{5}$$

Accordingly, the optimization function can be constructed as:

$$f = \min\{R(p), \delta^2, D(p) \le D\} \tag{6}$$

2.1.5 QoS route management module

The route management module is responsible for route installation, which proceeds as follows:

the route engine module collects route state information, which is loaded by the software-defined network (SDN) switch and forwarded with the packet.

2.2 Research Design of SDN Route Planning Study Based on AGAC Algorithm

2.2.1 QoS indicators

Constraint based QoS routing is to establish a routing path to reach the destination node starting from the source node and at the same time, the path satisfies the routing constraints for different services. Then the parameters of QoS are defined as follows:

Latency is:

$$D(r) = \sum_{e \in E(r)} Delay(e) \tag{7}$$

The bandwidth is:

$$B(r) = \min\{BandWidth(e), e \in E(r)\} \tag{8}$$

where: E is all communicable links, there exists a feasible link e between two nodes with $e \in E$; the path $r \in R$, R is the set of paths, and the set of edges of its path r is $E(r)$.

2.2.2 Genetic algorithm component

Route planning problem is essentially a problem of finding optimal solutions among multiple paths, genetic algorithm can find optimal solutions among a large number of solutions, applying genetic algorithm in route planning system can improve the convergence speed of large-scale network routing, and when dealing with multiple individuals in the population at the same time, it can evaluate the solutions and reduce the risk of falling into local optimal solutions.

(1) Chromosome coding

Chromosome coding uses priority coding technique, the coding for the selection of the next node with different priorities for node selection, the coding is different for each gene on the chromosome, with the characteristics of the arrangement of the coding.

(2) Calculation of fitness

The fitness function is used to determine the merit of the paths found, which has a significant impact on the algorithm's ability to find the optimal solution. According to the degree of impact of service on delay and bandwidth utilization, the paper solves for multiple feasible paths, and the fitness of path r_i is:

$$f(r_i) = \left(\delta \times D(r_i) + \varphi \times B(r_i)\right) \tag{9}$$

where: path $r_i \in R$, R is the set of path solution space; $D(r_i)$ is the delay of path r_i; $B(r_i)$ is the bandwidth occupancy of path r_i; and δ and φ are the influencing factors; the magnitude determines the degree of influence of the different service adaptations. .

(3) Selection operator

Selection operator is similar to the survival of the fittest in nature, the individuals with strong environmental adaptability are retained, otherwise they will be eliminated, and the excellent individuals are retained genetically by selection operator or the next generation of individuals is generated using crossover operator.

(4) Crossover operator

Sequential crossover is used to randomly select the genes of the two chromosomes in position crossover in order to generate new individuals.

(5) Variation operator

The main idea of this operator is to mutate the links that are relatively loaded or disconnected to make the links clear.

2.2.3 Ant colony algorithm

(1) Algorithm initialization

The maximum number of searches is $K_{\max}$, and the initial search time K is valued at 0. Assuming that the number of ants is M in total, the pheromones on all paths are initialized to be constant.

(2) Ant movement

Based on the pheromone concentration on the path and the link state, the ants are made to move to the next node by calculating the probability P_{ij}^k of all the reachable nodes.

$$P_{ij}^k = \begin{cases} \dfrac{\tau_{ij}^{\alpha}(t)\times\eta_{ij}^{\beta}(t)}{\sum\limits_{s\in allowed}\tau_{is}^{\alpha}(t)\times\eta_{is}^{\beta}(t)} & (j\in allowed) \\ 0 & (Other) \end{cases} \tag{10}$$

where: k is the sequence number of the ant; P_{ij}^k is the probability that ant k moves from the current node i to the feasible node j; α is the pheromone factor; β is the link parameter factor; $\tau_{ij}(t)$ is the pheromone concentration of the link between nodes i and j, $\eta_{ij}(t)$ is the visibility of the link between node i and j, and $allowed$ is the set of nodes that have not been visited yet.

(3) Updating pheromone

The pheromone update rule is:

$$\tau_{ij}(t+1)=\tau_{ij}(t)\times(1-\rho)+\Delta\tau_{ij}(t,t+1) \tag{11}$$

where: ρ is the pheromone volatilization factor; $1-\rho$ is the pheromone concentration attenuation coefficient; and $\Delta\tau_{ij}(t,t+1)$ is the pheromone content added on the path (i,j).

$$\Delta\tau_{ij}(t,t+1)=\sum_{k=1}^{m}\Delta\tau_{ij}^k(t,t+1) \tag{12}$$

where: $\Delta\tau_{ij}^k(t,t+1)$ is the pheromone content left by the kth ant on the path (i,j) in time $(t,t+1)$.

$$\Delta\tau_{ij}^k(t,t+1)=\frac{Q}{\delta\times D(r)_k+\varphi\times B(r)_k} \tag{13}$$

where: Q is the pheromone intensity; δ and φ are the influence factors; $D(r)_k$ is the delay of the k th ant that passes through the path in this loop; $B(r)_k$ is the bandwidth occupancy of the k th ant that passes through the path in this loop.

2.2.4 AGAC Algorithm Design

The main steps of AGAC algorithm are as follows:

(1) Initialization of the algorithm.

(2) Genetic algorithm simulates 5 evolutionary operations by selection, crossover and mutation to get 5 better paths.

(3) Record the 5 optimal specific paths and assign the pheromone equivalence to the corresponding paths in the pheromone matrix.

(4) Place M ants randomly on nodes in the network.

(5) Place the initial starting point of the ants in the set C, move each ant to the next vertex j, then add that path to the list of optional paths and add node j to the set C. Repeat the process until all ants have completed the traversal.

(6) Increase the number of loops, assign $K+1$ to K, and if $K = K_{\max}$, end the search and go to step (7); otherwise, update the pheromone concentration and return to step (4).

(7) Output the optimal path. This algorithm can reduce the original maximum number of searches and obtain the optimal path faster.

2.3 Results of AGAC algorithm in QoS routing

The parameters of the network are as follows: number of ants $m = 20$, $\alpha = 1$, $\beta = 2$, $\rho = 0.1$, $Q = 10$, $\tau_{\min} = 0.01$, $\tau_{\max} = 3$, $\mu 1 = 2$, $\mu 2 = 0.4$, $\lambda = 1$, $\theta 1 = 0.01$, $\theta 2 = 0.01$, $IterCount = 20$, $C = 6$, and maximum number of iterations $Nc = 300$. The network quality of service for each parameter $\left[B, D, j, P\right]$ is required to be $\left[40Mbps, 100ms, 40ms, 10e-3\right]$.

The following simulation experiments are performed for six routing requests. The basic ant colony algorithm, the maximum-minimum ant system, the freshness-based division of labor ant colony algorithm, and the algorithm of this paper (adaptive genetic ant colony algorithm) are used for the simulation experiments, the main parameters of the four algorithms are the same, and the number of algorithmic iteration loops is 300, and each group of experiments is run for 200 times in order to prevent the chance of intelligent search.

The experimental results of the basic ant colony algorithm are shown in Table 1; the experimental results of the max-min ant system are shown in Table 2; the experimental results of the freshness-based division of labor ant colony algorithm are shown in Table 3; and the experimental results of the adaptive genetic ant colony algorithm are shown in Table 4. It can be seen that the basic ant colony algorithm, the max-min ant system, and the two improved ant colony algorithms can achieve the optimal value in 200 experiments. The variance of multiple experiments shows that the variance of this paper's algorithm is smaller than that of the basic ant colony algorithm and the max-min ant system in each group of experiments, indicating that the difference between the solutions of adaptive genetic ant colony algorithm in each simulation experiment is relatively small, and the performance of the search for the optimum is relatively stable.

The average value of the routing cost and the ratio of the optimal solution in this paper's algorithm are both better than the basic ant colony algorithm and the max-min ant system. Although the average number of convergence of the basic ant colony algorithm is less than that of the max-min ant system and the adaptive genetic ant colony algorithm, the large number of experiments converge to the local optimum and become stagnant. The adaptive genetic ant colony algorithm is weaker than the max-min ant system in convergence performance, but its search performance is stronger than that of the max-min ant system and the basic ant colony algorithm; the difference between the freshness-based ant colony algorithm and the algorithm of this paper in terms of search performance is small.

Table 1: Experimental results of basic ant colony algorithm

Originating node	Destination node	Optimal solution path cost	Worst-case path cost	Average value	Optimal solution ratio	Variance	Average Iteration Count
5	35	34.88	51.76	38.537	0.0166	3.4324	15.685
3	32	35.35	36.26	33.340	0.2606	2.5449	19.49
5	36	29.16	48.8	35.161	0.0301	12.8027	15.005
3	36	36.07	48.2	44.538	0.0195	4.8395	24.96
2	27	33.09	42.83	37.491	0.0385	5.4545	26.355
5	35	26.17	37.47	31.958	0.1804	8.3052	13.275

Table 2: Experimental results of the maximum-minimum ant system

Originating node	Destination node	Optimal solution path cost	Worst-case path cost	Average value	Optimal solution ratio	Variance	Average Iteration Count
5	35	34.88	32.86	32.859	0.5207	0.7188	95.2
3	32	35.35	34.96	30.711	0.6475	0.6138	37.265
5	36	29.16	38.31	27.235	0.5311	0.9351	94.89
3	36	36.07	43.38	37.954	0.5567	1.1673	68.05
2	27	33.09	37.64	31.133	0.1913	0.3935	75.345
5	35	26.17	34.34	28.595	0.8414	1.0845	48.99

Table 3: Result of Division of Labor Ant Colony Algorithm Based on Freshness

Originating node	Destination node	Optimal solution path cost	Worst-case path cost	Average value	Optimal solution ratio	Variance	Average Iteration Count
5	35	34.88	36.18	34.375	0.7246	0.5304	131.16
3	32	35.35	31.85	31.484	0.9643	0.0105	97.195
5	36	29.16	31.41	28.845	0.8639	0.1777	109.68
3	36	36.07	39.85	37.525	0.6879	0.3317	90.89
2	27	33.09	36.34	32.417	0.5008	0.2373	105.45
5	35	26.17	30.99	27.135	0.9181	0.0832	76.095

Table 4: Results Based on Adaptive Genetic Ant Colony Algorithm

Originating node	Destination node	Optimal solution path cost	Worst-case path cost	Average value	Optimal solution ratio	Variance	Average Iteration Count
5	35	34.88	35.29	33.037	0.7959	0.1826	108.36
3	32	35.35	33.21	30.405	0.9671	0.0119	56.17
5	36	29.16	31.43	28.719	0.9107	0.0289	78.05
3	36	36.07	37.06	34.904	0.9363	0.0553	83.86

2	27	33.09	32.05	31.174	0.5204	0.0572	94.5
5	29	26.17	30.22	27.797	0.9806	0.0249	57.75

Taking the experimental routing requests (5-35),(3-32),(2-27) as examples, we analyze the average evolution curves of the global optimal solutions of routing sought by the three algorithms for 200 experiments. The average optimal evolution curve of the requested routing cost is shown in Fig. 1, where (a)~(c) represent the three kinds of routing requests 5-35, 3-32 and 2-27, respectively. It can be seen that: the average value of the global optimal cost of routing sought by the adaptive genetic ant colony algorithm in each round of iterative loops in multiple experiments obtains better results than the basic ant colony algorithm with the max-min ant system in the process of evolution.

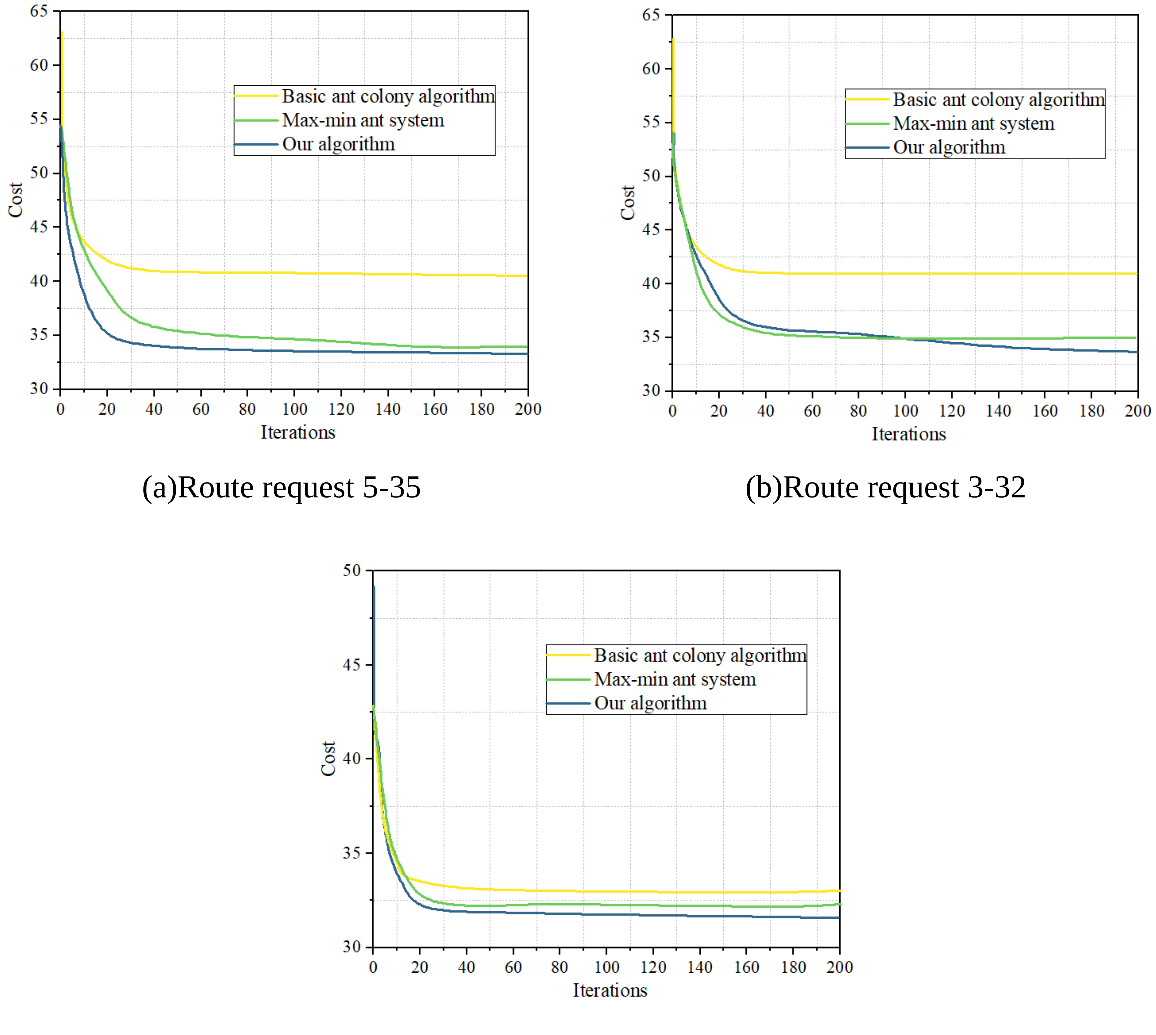

(a)Route request 5-35

(b)Route request 3-32

(c)Route request 2-27

Figure 1: Average optimal evolution curve of the requested route cost

Taking the route request source node s=3 and destination node d=36 as an example,the evolution results of the three ant colony algorithms are obtained as shown in Fig. 2. It can be seen that the adaptive genetic ant colony algorithm is able to search for routing solutions with lower cost than the basic ant colony algorithm and the max-min ant system. The basic ant colony algorithm falls into stagnation and converges to the local optimum, and the adaptive genetic ant colony algorithm searches for the routing cost better than the max-min ant system, but the convergence performance is slightly worse than the max-min ant system.

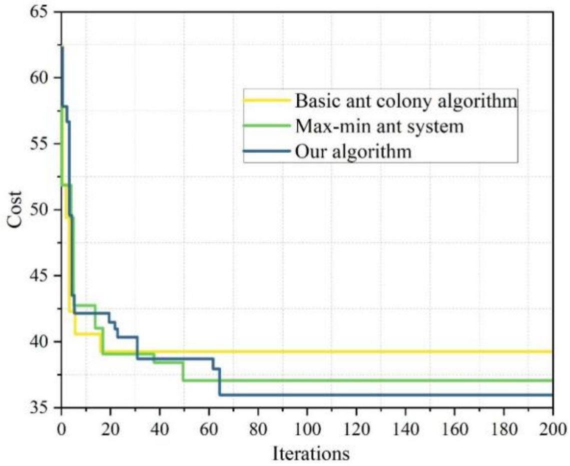

Figure 2: Evolutionary Results of Three Ant Colony Algorithms

The results of delay evolution under the optimal cost conditions of the three ACO algorithms and the results of delay jitter evolution under the optimal cost conditions of the three ACO algorithms are shown in Figs. 3 and 4, respectively. It can be seen that the routing solutions obtained by the three ACO algorithms can satisfy the QoS attribute constraints.

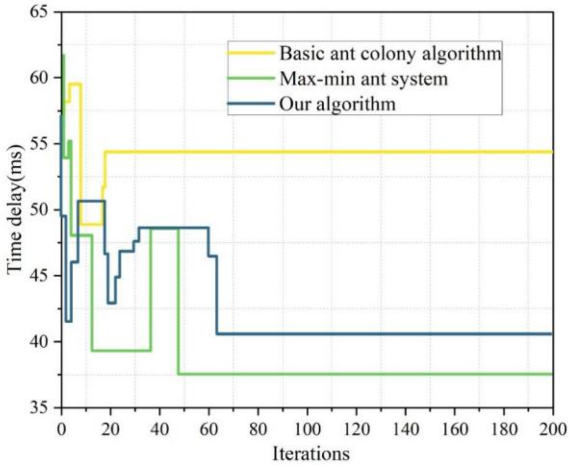

Figure 3: The Evolution of Delay under the Condition of Optimal Cost

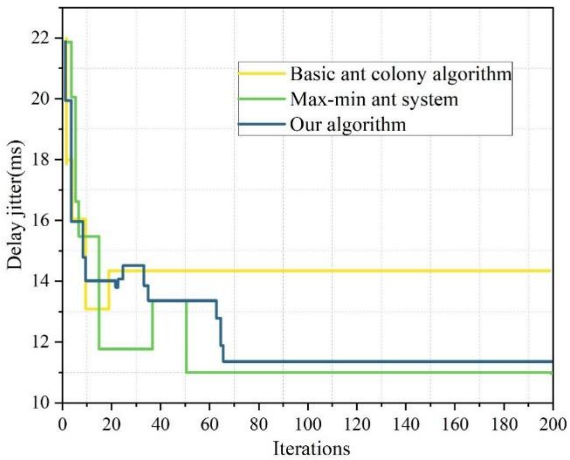

Figure 4: Evolution of delay jitter under optimal cost condition

Taking the routing requests (2-27),(3-32),(5-29),(5-36) as an example, the search results of the four algorithms are compared and analyzed when the pheromone-inspired factor takes different values and the other parameters are the defaults of the experiments in this chapter. The experimental results of the four algorithms when the pheromone-inspired factor takes different values are shown in Table 5.IACO is the freshness-based division of labor ant colony algorithm, and AGAC is the adaptive genetic ant colony algorithm. It can be seen that the search performance of this paper's algorithm is better than the other three comparative algorithms when the pheromone heuristic factor takes different parameter values.

Table 5: Results of different algorithms with different pheromone inspiration factor

Route request	Algorithm	1	2	3
2-27	ACO	35.046	35.840	37.203
	MMAS	32.259	34.539	35.249
	IACO	31.527	31.434	31.660
	AGAC	31.687	30.219	30.271
3-32	ACO	37.643	39.640	40.757
	MMAS	34.481	35.676	37.925
	IACO	32.740	32.853	33.114
	AGAC	31.966	31.539	32.201
5-29	ACO	35.979	37.177	39.059
	MMAS	30.267	31.132	33.402
	IACO	28.123	28.083	28.566
	AGAC	27.297	27.192	27.808
5-36	ACO	40.145	40.669	46.938
	MMAS	36.333	37.408	39.660
	IACO	33.398	33.399	34.250
	AGAC	32.407	32.867	33.418

3 Research on fault node monitoring of power distribution network based on optimized genetic algorithm

3.1 Distribution network fault location algorithm based on optimized genetic algorithm

3.1.1 Genetic Algorithm Ideas for Distribution Network Fault Localization

(1) Parameter encoding

The input parameter of the genetic algorithm is the fault overcurrent signal detected by the FTU, and the output parameter is the line state of the distribution network based on segmentation. The line is divided into 2 states, normal and fault, and the switch is divided into 2 cases, overcurrent and no overcurrent, which can be seen that these 2 parameters are discrete quantities with obvious characteristics, so they are encoded in binary. Assuming that the line normal and switch no overcurrent are represented by 0, the line fault or switch overcurrent is represented as:

$$\begin{cases} 0 & \text{Circuit normal, switch without overcurrent} \\ 1 & \text{Circuit fault, switch overcurrent} \end{cases} \tag{14}$$

(2) Switching Function and Adaptation Function

The essence of the switching function is to map the switch state to the associated line state and expresses the relationship between the distribution line and the switch in a discretized digital quantity. Switching function:

$$I'_m(s) = \prod_n S_n \tag{15}$$

The value of the switching function is either 0 or 1. Π denotes the logical or operation, and S_n denotes the state of the nth segment of the distribution line associated with switch m.

The fitness function of the construction algorithm is derived as:

$$F(s) = \sum_{m=1}^{N} \left| I_m - I'_m(s) \right| \tag{16}$$

The I_m is acquired by the metering automation system in real time. When the mth switch collects the fault current signal, I_m is 1, otherwise it is 0. Based on the calculation of the fitness, the search for the optimal solution group becomes the search for the solution group with the smallest fitness, and the line corresponding to the solution with the smallest fitness value coded as 1 in the optimal solution group is the fault line.

(3) Genetic operation

In genetic operation, individual selection, individual crossover, and individual mutation operations are used to realize the convergence of fitness in the solution space and the purpose of population diversification.

The selection operation is to select the solution with the highest fitness and store it in the matching set. Except for the 10% solutions with the highest fitness, the rest of the solutions stored in the matching set need to satisfy:

$$\begin{cases} \sum_{i=1}^{m-1} f_i < r \\ \sum_{i=1}^{m} f_i > r \end{cases} \tag{17}$$

The crossover operation is based on the crossover operator to crossover the individuals in the matched set. The larger the crossover operator, the larger the crossover rate, meaning that more individuals will be crossed. When the crossover rate is too large, it makes the likelihood that individuals with higher fitness values will be corrupted will increase, and vice versa, it will make the iterative process of the algorithm too slow.

3.1.2 Optimization of genetic algorithms

(1) Parameter coding optimization

The tendency of the distribution network structure to be distributed and the complexity of the feeder topology can lead to different directions of fault currents. Therefore, it is necessary to define the parameters based on the reference positive direction determined by the switch. The fault current in the same direction as the reference positive direction is 1, the fault current in the opposite direction of the reference positive direction is -1, and no fault current is 0. The state of the line is still indicated by 0 and 1 for normal and fault.

(2) Improvement of switching function

When the distribution network structure becomes distributed, the switching function of the traditional genetic algorithm cannot correctly express the correlation relationship between lines and switches. Therefore, this paper introduces the association operator of distributed power supply to improve the traditional switching function. The reconstructed switching function is:

$$I'_j(s)=\left(\prod_{i=1}^{N} D_{G_i}\right)\times\left[0-\left(\prod_{s=1}^{A} S_{j_s}\right)\right]+\left(\prod_{x=1}^{B} S_{j_d}\right) \tag{18}$$

D_{G_i} is the distributed coefficient, which takes the value of 1 if the corresponding distributed power source starts grid-connected generation, and 0 otherwise; The S_s indicates the fault status of distribution line s, with a fault of 1 and vice versa; $\prod_{s=1}^{A} S_{j_s}$ denotes the result of the calculation of the logical or of all distribution line fault states along the reference negative direction to the power source for the j th FTU; S_{j_d} denotes the fault state of distribution line d, where fault is 1 and vice versa; $\prod_{d=1}^{B} S_{j_d}$ denotes the result of the computation of the logical or of all the fault states of the distribution line along the positive direction of reference for the j FTU.

(3) Optimization of adaptation function

Based on the improved switching function, combined with the theory of minimum set for fault diagnosis, the adaptation degree function is optimized to obtain:

$$F(S)=\sum_{m=1}^{N}\left|I_m-I'_m(s)\right|+\left|\sum_{i=1}^{N} S_i-\partial\right| \tag{19}$$

The misjudgment factor $\sum_{i=1}^{N} S_i$ is introduced in Eq. to prevent misjudgment in the algorithm results, which represents the sum of line fault states. At the same time, the leakage judgment parameter ∂ is added to prevent the algorithm results from leakage judgment.

(4) Optimize the flow of genetic algorithm

The optimized flow of the algorithm is shown in Figure 5. In order to make the algorithm more adaptable to the actual situation of distribution network faults are mostly single point faults, the population is initialized based on single point faults, which is more helpful to improve the convergence efficiency of the genetic algorithm.

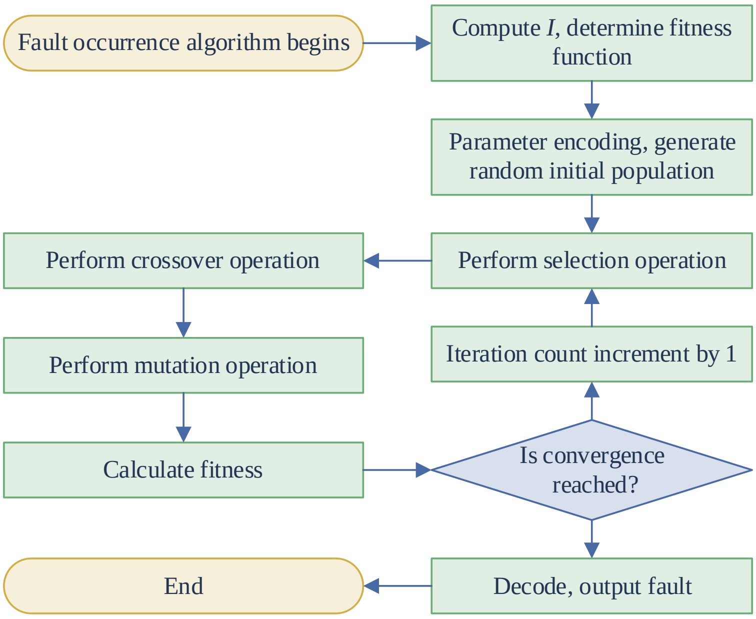

Figure 5: Optimize the genetic algorithm process

3.2 Analysis of power distribution network fault node monitoring results

3.2.1 Example of a distribution network with open-loop operation of two power sources

Take the dual power supply open-loop operation distribution network as an example to illustrate the algorithm realization process, and the dual power supply distribution network wiring is shown in Fig. 6.

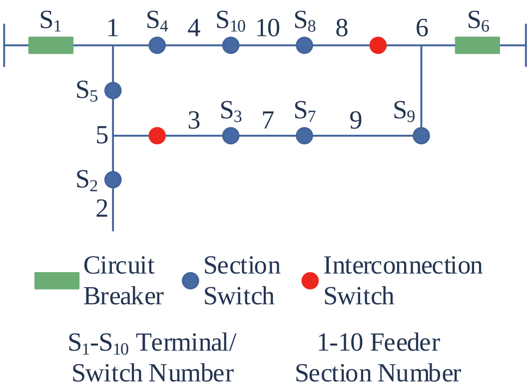

Figure 6: Wiring of dual power supply distribution network

It is assumed that zone 6 is faulty and the fault information is sound. The algorithm parameters are set as follows: population size $N=10$, antibody coding length $D=10$; learning factor $c_1=c_2=1.5031$, antibody similarity evaluation parameter $e=0.9$; adaptive inertia weight ω is set, and the value is reduced stepwise by the number of algorithm iterations $\omega\in[0.4,0.9]$; the maximum number of iterations of the algorithm $k_{\max}=20$.

The algorithm first generates the initial antibody population and velocity vectors, forms a memory cell bank $(N_m=2)$, and calculates the individual and global extreme points; second, the antibody code and velocity vectors are updated, and N_t antibodies are randomly generated

$(N_t = 2)$ to obtain the temporary antibody population X_t; Calculate the antibody affinity and concentration of the temporary antibody population to determine the antibody selection probability. The antibodies and their parameters of the first iteration are shown in Table 6, which contains the antibody code, affinity, concentration, and selection probability of the temporary antibody population and the memory cell library at the first iteration. Based on the switch function and fitness function selection and affinity correction rules, antibodies 2~11 were selected to obtain promotion, replacing antibody 1 with antibody 12 for affinity correction with memory antibodies, updating individual polarity and global polarity, and entering the second iteration.

Table 6: The first-generation antibody and its parameters

Antibody number	Code	Affinity	P_{ai}	Potency	P_{di}
1	0010010100	0.1175	0.0669	0.0799	0.0684
2	1101100010	0.1999	0.1150	0.0834	0.0710
3	0000100101	0.1318	0.0755	0.0831	0.0704
4	1111011000	0.1419	0.0792	0.0823	0.0731
5	0000111010	0.1541	0.0835	0.0823	0.0687
6	0110000011	0.1197	0.0666	0.0826	0.0727
7	0000011000	0.1658	0.0942	0.1667	0.1414
8	0001101101	0.1325	0.0744	0.1670	0.1420
9	1010000001	0.1160	0.0652	0.0834	0.0714
10	0100101000	0.2819	0.1595	0.0806	0.0722
11	1011000010	0.1259	0.0693	0.0837	0.0721
12	0001010101	0.1055	0.0574	0.0845	0.0702
Memory antibody	0010101010	0.2914	—	—	—
Memory antibody	0101100110	0.2033	—	—	—

The antibodies and their parameters for the second iteration are shown in Table 7. The results show that the optimal antibody, i.e., antibody 2, appears in the second iteration, and the algorithm stores the memory optimized by the switching function and the fitness function into the memory cell library. After the completion of the algorithm iteration, the optimal antibody [0 0 0 0 0 1 0 0 0 0] is output, and the feeder segment 6 is determined as a faulty segment.

Table 7: The second-generation antibody and its parameters

Antibody number	Code	Affinity	P_{ai}	Potency	P_{di}
1	0001000000	0.2873	0.0394	0.4188	0.0833
2	0000010000	2.0000	0.2766	0.5012	0.0995
3	0000000000	0.4990	0.0710	0.5829	0.1162
4	0100000000	0.6633	0.0929	0.5830	0.1159
5	1000000000	0.5004	0.0690	0.5841	0.1160
6	0010010000	0.6686	0.0675	0.3354	0.0654
7	0000100000	0.5020	0.0677	0.5822	0.1159
8	0100000010	0.2017	0.0284	0.2502	0.0507
9	0010100000	0.9990	0.1399	0.2503	0.0489
10	0100000100	0.6668	0.0926	0.5813	0.1155
11	1000100000	0.2214	0.0279	0.1673	0.0343
12	0000011000	0.1672	0.0254	0.1631	0.0325
Memory antibody	0010101010	0.2914	—	—	—
Memory antibody	0101100110	0.2033	—	—	—

3.2.2 Simulation testing of complex distribution systems

The IEEE33 feeder segment distribution system is used as an example to verify the effectiveness of the algorithm proposed in this paper.The network wiring of the IEEE33 feeder segment distribution system is shown in Fig. 7. Set the population size $N = 100$, the antibody coding length $D = 33$, the maximum number of iterations $k_{\max} = 50$, and other parameters are set unchanged.

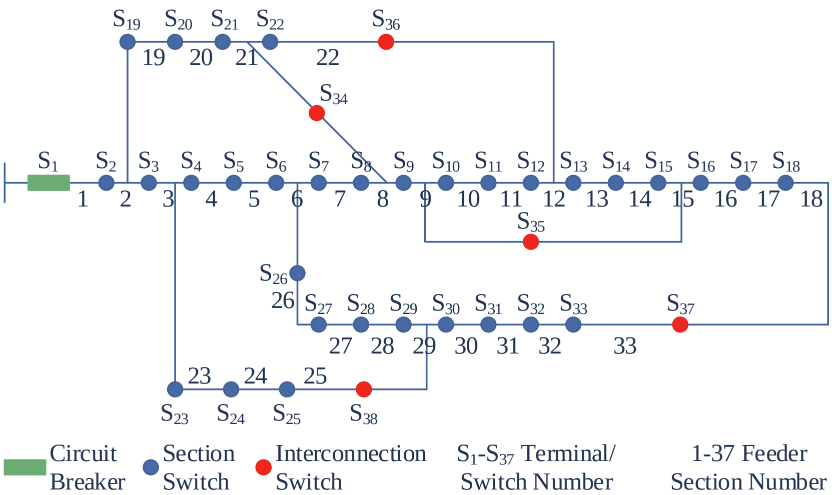

Figure 7: IEEE33 Feeder Section Distribution System Network Connection

The effectiveness of the algorithm is verified in the Matlab simulation environment. In view of the large number of fault situations, representative typical examples are selected for testing in the simulation, which cover different fault locations in the distribution network as well as a variety of fault situations such as single fault, multiple faults, sound fault information, fault information distortion, and so on, and the test results are shown in Table 8. The simulation results show that the algorithm proposed in this paper can quickly and accurately locate the fault section under various fault situations, such as single fault, multi-point fault, feeder end fault, etc., and has strong fault tolerance when the fault information is distorted.

Table 8: Test result

Hypothesis of fault location	Distortion terminal number	Fault section	Location result
13	No	13	Exactness
20	S6	20	Exactness
23	S8, S17	23	Exactness
31	S15, S22, S28	31	Exactness
17	S3, S11, S22, S32	17	Exactness
5,22	No	5, 22	Exactness
12,28	S3	12, 28	Exactness
16,34	S5, S18	16, 34	Exactness
24,35	S4, S15, S25	24, 35	Exactness
25,30	S5, S10, S15, S33	25, 30	Exactness
16,25,29	No	16, 25, 29	Exactness
18,26,28	S23	18, 26, 28	Exactness
17,28,31	S14, S18	17, 28, 31	Exactness
10,23,26	S3, S14, S22	10, 23, 26	Exactness

3.2.3 Performance comparison of algorithms

In order to show the performance advantages of the algorithm proposed in this paper, the following 2 typical convergence conditions are used to compare and test the IBPSO algorithm with the BPSO algorithm, and the parameter settings of the BPSO algorithm are the same as those of the IBPSO algorithm.

Convergence condition 1: The algorithm reaches the maximum number of iterations. The simulation is run 20 times for the case of zone 20 fault without information distortion and the case of node 6 and 8 fault with information distortion, and the average affinity fitness change curve of the algorithm is plotted to test the convergence performance, and the results of the algorithm's affinity change in the case of information soundness and information distortion are shown in Fig. 8, in which (a) and (b) represent the two cases of information soundness and information distortion, respectively. It can be seen that the optimized genetic algorithm (IBPSO) and the pre-optimization genetic algorithm (BPSO) can accurately locate the faults under the maximum number of iterations of the convergence condition. However, due to the optimization of the algorithm through the introduction of the switch function and the fitness function, the memory link effectively improves the quality of the individuals of the antibody population after the updating, and thus the number of iterations of the global optimal solution of IBPSO is significantly lower than that of the algorithm of IBPSO. The number of iterations of IBPSO is significantly less than that of BPSO, which has a greater advantage in the convergence speed of the algorithm.

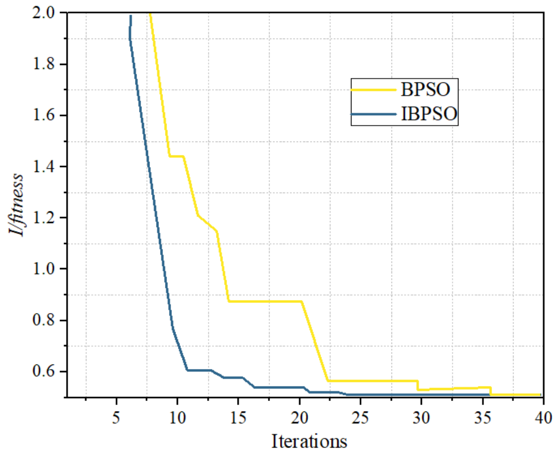

(a) Information is sound

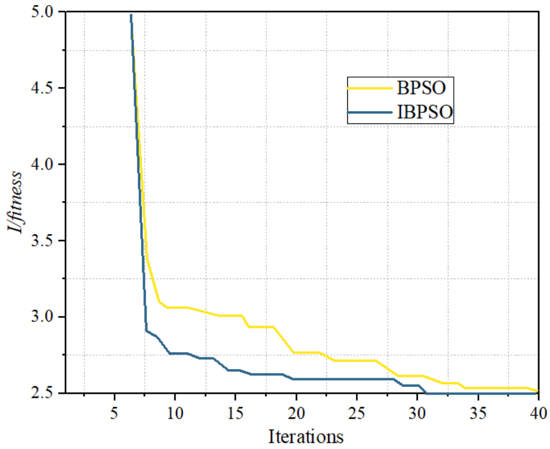

(b) Information distortion

Figure 8: Algorithm affinity change results

Convergence condition 2: global extreme point is not updated for 5 consecutive times. The simulation is run 50 times under various fault scenarios such as single fault, multi-point fault, information soundness, information distortion, etc. in the network, and the number of correct localization and the average number of iterations of the statistical algorithm, and the experimental comparison results under the convergence condition 2 are shown in Table 9. The results show that when the convergence condition of the algorithm is set to the global extreme point without updating for six consecutive times, the number of correct times and the average number of iterations of fault localization of the IBPSO algorithm optimized based on the switching function and the fitness function are significantly better than that of the BPSO algorithm.

Table 9: Experimental comparison results under the condition of convergence

Fault region	Distortion position	Average Iteration Count		Correct attempts	
		BPSO	IBPSO	BPSO	IBPSO
20	No	24.22	15.67	32	49
18,34	No	24.95	15.73	26	44
14	26	23.65	15.89	34	51
29	5,12,27	24.05	15.37	30	43
17,33	22,32	24.24	16.56	27	43

4 Conclusion

In this paper, we first propose a QoS-ensure traffic control strategy to solve the defects of low routing efficiency and poor data processing capability of traditional grid data center network; then we design a real-time route planning framework based on software-defined network (SDN) to improve the data transmission problem that traditional routing algorithms can not satisfy the demand of different business quality of service (QoS). Finally, an optimized genetic algorithm for fault localization in distribution networks is proposed to solve the problems of poor adaptability and poor interference resistance of genetic algorithms. The results show that:

(1) The variance of the adaptive genetic ant colony algorithm (AGAC) proposed in this paper is much lower than that of the three comparative algorithms, and the difference of the solutions obtained in each simulation experiment is smaller, and the performance of the algorithm in searching for optimization is more stable. In addition, the algorithm minimizes the average value of the global optimal cost of the routes in each iteration loop, and the obtained routing solution can satisfy the QoS attribute constraints, and still obtains better results with different parameter values of the pheromone heuristic factor.

(2) Compared with the BPSO algorithm, the improved IBPSO has a greater advantage in convergence speed and fault localization accuracy, and it has a stronger fault-tolerance performance in the case of information distortion.

About the Author

Wenqiang Zou (1994.7-), male, Han ethnicity, from Guiyang, Guizhou Province, holds a bachelor's degree and works as an engineer specializing in production command and technical management.

Kunhua Yang (1995.11-), male, of Dong ethnicity, is a master's degree holder and engineer from Tianzhu, Guizhou Province. His research focuses on digital production business.

Yuchuan Deng (1994.6-), male, Han ethnicity, from Guiyang, Guizhou Province, holds a bachelor's degree and works as an engineer specializing in ubiquitous power marketing solutions.

Xuan'an Lin (1996.11-), female, Miao ethnicity, native of Tianzhu, Guizhou Province, holds a bachelor's degree and works as an engineer specializing in ubiquitous device operation monitoring and data asset management.

Ying Deng (1994.8-), female, Han ethnicity, from Guiyang, Guizhou Province, holds a bachelor's degree and works as an assistant engineer specializing in ubiquitous power distribution operations.

References

[1] Deng, F., Zu, Y., Mao, Y., Zeng, X., Li, Z., Tang, X., & Wang, Y. (2020). A method for distribution network line selection and fault location based on a hierarchical fault monitoring and control system. International Journal of Electrical Power & Energy Systems, 123, 106061.

[2] Adewole, A. C., Tzoneva, R., & Behardien, S. (2016). Distribution network fault section identification and fault location using wavelet entropy and neural networks. Applied soft computing, 46, 296-306.

[3] Gu, J. C., Huang, Z. J., Wang, J. M., Hsu, L. C., & Yang, M. T. (2020). High impedance fault detection in overhead distribution feeders using a DSP-based feeder terminal unit. IEEE Transactions on Industry Applications, 57(1), 179-186.

[4] Shu, H., Wang, B., Dong, J., & Tang, Y. (2025). Fault location in the observation matrix of collection lines for grid-connected wind power supported by grid-forming energy storage. International Journal of Electrical Power & Energy Systems, 172, 111226.

[5] Wang, C., Zhang, T., Luo, F., Li, P., & Yao, L. (2018). Fault incidence matrix based reliability evaluation method for complex distribution system. IEEE Transactions on Power Systems, 33(6), 6736-6745.

[6] Li, Z., Qiao, J., Wang, Y., & Yin, X. (2022). A comprehensive method for fault location of active distribution network based on improved matrix algorithm and optimization algorithm. International Transactions on Electrical Energy Systems, 2022(1), 4232090.

[7] Dashti, R., Ghasemi, M., & Daisy, M. (2018). Fault location in power distribution network with presence of distributed generation resources using impedance based method and applying π line model. Energy, 159, 344-360.

[8] Hosseinimoghadam, S. M. S., Dashtdar, M., & Dashtdar, M. (2021). Fault location in distribution networks with the presence of distributed generation units based on the impedance matrix. Journal of The Institution of Engineers (India): Series B, 102(2), 227-236.

[9] Hamatwi, E., Imoru, O., Kanime, M. M., & Kanelombe, H. S. (2023). Comparative analysis of high impedance fault detection techniques on distribution networks. IEEE Access, 11, 25817-25834.

[10] Mortazavi, H., Mehrjerdi, H., Saad, M., Lefebvre, S., Asber, D., & Lenoir, L. (2016). An impedance-based method for distribution system monitoring. IEEE Transactions on Smart Grid, 9(1), 220-229.

[11] Aftab, M. A., Hussain, S. S., Ali, I., & Ustun, T. S. (2020). Dynamic protection of power systems with high penetration of renewables: A review of the traveling wave based fault location techniques. International Journal of Electrical Power & Energy Systems, 114, 105410.

[12] Kong, B., Liu, B., Liu, X., Pu, B., Feng, J., & Zeng, X. (2020). Analysis of traveling wave based fault location method for distribution network with image processing.

Vibroengineering Procedia, 31, 21-26.

[13] Qin, X., Wang, P., Liu, Y., Guo, L., Sheng, G., & Jiang, X. (2017). Research on distribution network fault recognition method based on time-frequency characteristics of fault waveforms. IEEE Access, 6, 7291-7300.

[14] Izadi, M., & Mohsenian-Rad, H. (2021). Synchronous waveform measurements to locate transient events and incipient faults in power distribution networks. IEEE Transactions on Smart Grid, 12(5), 4295-4307.

[15] Jiang, Q., Huang, B., Ding, S. X., & Yan, X. (2016). Bayesian fault diagnosis with asynchronous measurements and its application in networked distributed monitoring. IEEE Transactions on Industrial Electronics, 63(10), 6316-6324.

[16] Zhu, J., Mu, L., Ma, D., & Zhang, X. (2021). Faulty line identification method based on bayesian optimization for distribution network. IEEE Access, 9, 83175-83184.

[17] Cai, B., Liu, Y., & Xie, M. (2016). A dynamic-Bayesian-network-based fault diagnosis methodology considering transient and intermittent faults. IEEE Transactions on Automation Science and Engineering, 14(1), 276-285.

[18] Jiang, K., Wang, H., Shahidehpour, M., & He, B. (2021). Block-sparse Bayesian learning method for fault location in active distribution networks with limited synchronized measurements. IEEE Transactions on Power Systems, 36(4), 3189-3203.

[19] Wang, Y., Wang, T., & Liu, L. (2023). A fault segment location method for distribution networks based on spiking neural P systems and Bayesian estimation. Protection and Control of Modern Power Systems, 8(3), 1-12.

[20] Mnyanghwalo, D., Kundaeli, H., Kalinga, E., & Hamisi, N. (2020). Deep learning approaches for fault detection and classifications in the electrical secondary distribution network: Methods comparison and recurrent neural network accuracy comparison. Cogent Engineering, 7(1), 1857500.

[21] Mirshekali, H., Dashti, R., Keshavarz, A., & Shaker, H. R. (2022). Machine learning-based fault location for smart distribution networks equipped with micro-PMU. Sensors, 22(3), 945.

[22] Baghaee, H. R., Mlakić, D., Nikolovski, S., & Dragicević, T. (2019). Support vector machine-based islanding and grid fault detection in active distribution networks. IEEE Journal of Emerging and Selected Topics in Power Electronics, 8(3), 2385-2403.

[23] Rizeakos, V., Bachoumis, A., Andriopoulos, N., Birbas, M., & Birbas, A. (2023). Deep learning-based application for fault location identification and type classification in active distribution grids. Applied Energy, 338, 120932.

[24] Maruf, H. M., Müller, F., Hassan, M. S., & Chowdhury, B. (2018, June). Locating faults in distribution systems in the presence of distributed generation using machine learning techniques. In 2018 9th IEEE International Symposium on Power Electronics for Distributed Generation Systems (PEDG) (pp. 1-6). IEEE.

[25] Gülmez, E., Koruca, H. I., Aydin, M. E., & Urganci, K. B. (2024). Heuristic and swarm intelligence algorithms for work-life balance problem. Computers & Industrial Engineering, 187, 109857.

[26] Bi, Z., Yang, X., Wang, B., Zhang, W., Dong, Z., & Zhang, D. (2023). Quantum annealing algorithm for fault section location in distribution networks. Applied Soft Computing, 149, 110973.

[27] Kahouli, O., Alsaif, H., Bouteraa, Y., Ben Ali, N., & Chaabene, M. (2021). Power system reconfiguration in distribution network for improving reliability using genetic algorithm and particle swarm optimization. Applied Sciences, 11(7), 3092.

[28] Wen, J., Qu, X., Liu, J., Lin, S., & Xiao, Q. (2024). A novel fault location method for the active distribution network based on dynamic quantum genetic algorithm. Electrical Engineering, 106(4), 4719-4735.

[29] Recioui, A. E. M., Merdj, M., & Kamli, A. (2021). Optimal placement of fault passage indicators in distribution networks using genetic algorithms. Algerian Journal of Signals and Systems, 6(4), 181-191.